




Photobiomodulation Therapy Attenuates Hypoxic-Ischemic Injury in a Neonatal Rat Model

Lorelei Donovan Tucker¹ · Yujiao Lu¹ · Yan Dong¹ · Luodan Yang¹ · Yong Li¹ · Ningjun Zhao¹ · Quanguang Zhang¹ 

Received: 30 April 2018 / Accepted: 11 July 2018 / Published online: 22 July 2018
© Springer Science+Business Media, LLC, part of Springer Nature 2018, corrected publication August/2018

Abstract

Photobiomodulation (PBM) has been demonstrated as a neuroprotective strategy, but its effect on perinatal hypoxic-ischemic encephalopathy is still unknown. The current study was designed to shed light on the potential beneficial effect of PBM on neonatal brain injury induced by hypoxia ischemia (HI) in a rat model. Postnatal rats were subjected to hypoxic-ischemic insult, followed by a 7-day PBM treatment via a continuous wave diode laser with a wavelength of 808 nm. We demonstrated that PBM treatment significantly reduced HI-induced brain lesion in both the cortex and hippocampal CA1 subregions. Molecular studies indicated that PBM treatment profoundly restored mitochondrial dynamics by suppressing HI-induced mitochondrial fragmentation. Further investigation of mitochondrial function revealed that PBM treatment remarkably attenuated mitochondrial membrane collapse, accompanied with enhanced ATP synthesis in neonatal HI rats. In addition, PBM treatment led to robust inhibition of oxidative damage, manifested by significant reduction in the productions of 4-HNE, P-H2AX (S139), malondialdehyde (MDA), as well as protein carbonyls. Finally, PBM treatment suppressed the activation of mitochondria-dependent neuronal apoptosis in HI rats, as evidenced by decreased pro-apoptotic cascade 3/9 and TUNEL-positive neurons. Taken together, our findings demonstrated that PBM treatment contributed to a robust neuroprotection via the attenuation of mitochondrial dysfunction, oxidative stress, and final neuronal apoptosis in the neonatal HI brain.

Keywords Photobiomodulation therapy · Neonatal hypoxic-ischemia · Apoptosis · Mitochondrial dysfunction · Oxidative stress

Introduction

Occurring in ~0.4% of live births and presenting a mortality rate of 20%, neonatal hypoxic ischemic encephalopathy (HIE) is a major cause of mortality and morbidity in newborn infants (Colver et al. 2014; Juul and Ferriero 2014), occurring most commonly in premature infants (Vannucci and Hagberg 2004). Hypoxic ischemia (HI) commences during birth or in the early perinatal period with a reduction or cessation of cerebral blood flow, resulting in hypoxic brain injury that causes white matter necrotic lesions and dispersed gray matter apoptosis (Blomgren and Hagberg 2006). The damage left in the wake of neonatal HI contributes heavily to infant mortality, as well as several motor and developmental disorders that

generally persist throughout adulthood. The most well-known of these conditions is spastic cerebral palsy, a disabling condition characterized by physical disability and long-term developmental difficulties, of which HIE is the primary cause. In mild to moderate cases, however, HI damage may manifest in adolescence as cognitive, attentional, and behavioral disturbances that appear seemingly without cause (Blomgren and Hagberg 2006; Semple et al. 2013). This is of particular significance, as modern developments in postnatal healthcare have decreased incidence of the most severe cases, whereas mild to moderate cases occur with startling frequency (Smith et al. 2000). HIE is heavily associated with low birth weight and demands immediate postnatal intensive care (Vannucci and Hagberg 2004). Compounding this problem is the stark lack of effective therapeutic options that can slow the advance of ischemic injury in the neonatal brain.

In many ways, the neonatal ischemic response reflects that of the mature brain. Reduced O₂ levels decrease aerobic respiration, causing a sharp decline in neuronal ATP levels. Without the ATP required for maintenance of the resting neuronal transmembrane potential, widespread depolarization occurs, triggering widespread excessive glutamate release (Vannucci and Hagberg 2004; Thornton et al. 2012). This

Lorelei Donovan Tucker and Yujiao Lu contributed equally to this work.

✉ Quanguang Zhang
qzhang@augusta.edu

¹ Department of Neuroscience and Regenerative Medicine, Medical College of Georgia, Augusta University, 1120 15th Street, Augusta, GA 30912, USA

released glutamate acts on receptors of postsynaptic cells, triggering excessive firing that strengthens inappropriate circuits, potentially leading to long-lasting pathologies of severe epilepsy due to developmental upregulation of NMDA receptor subunits (Vannucci and Hagberg 2004; Semple et al. 2013). Glutamatergic excitatory signaling initiates rapid over-influx of Ca^{2+} , contributing to activation of mitochondrial apoptosis pathways (Thornton et al. 2012). Alongside this, Ca^{2+} influx triggers cellular production of reactive oxygen species (ROS) that initiate cellular damage in HI (Blomgren and Hagberg 2006). Peroxynitrite, in particular, causes excessive lipid peroxidation that contributes significantly to the pathology of HI injury, especially damage to immature oligodendrocytes and their progenitors (Blomgren and Hagberg 2006). This contributes to and is simultaneously exacerbated by developing mitochondrial damage, resulting in sporadic cell death, particularly in sensitive and developmentally critical pools of neural progenitor cells (Vannucci and Hagberg 2004). These insults impact the population, proliferation, and differentiation of these cells, resulting in impaired development with repercussions lasting a lifetime (Semple et al. 2013; Rumajogee et al. 2016). During this process, mitochondrial function is compromised, which contributes heavily to the long-term pathophysiology of neonatal HI injury.

The mitochondria are highly dynamic organelles that play vital roles in oxidative energy metabolism and cellular signaling. During the process of oxidative phosphorylation that produces critical cellular ATP, the mitochondria shuttle highly-energetic electrons from food substrates along a series of protein complexes, the electron transfer chain (ETC). Blockade of this process leads to electron leakage that produces dangerous free radicals which damage mitochondrial components, initiating a self-perpetuating cycle that prolongs the impact of the initial insult over an extended duration (Akbar et al. 2016; Ham and Raju Ham 3rd and Raju 2017). The dysfunction can translate into long-term deficits in mitochondrial function and energy production (Akbar et al. 2016). In addition, mitochondrial dysfunction disrupts the mitochondrial dynamics that mitochondria rely on, resulting in widespread mitochondrial fragmentation. Mitochondrial fission and fusion events, referred to as mitochondrial dynamics, maintain function via repair and mitochondrial quality control, with fusion events facilitating sharing of mitochondrial components, and fission allowing for mitophagy of poorly functioning mitochondrial fragments, determined by the mitochondrial membrane potential (MMP). The balance between these competing forces is vital for mitochondrial function, and disturbances in this process are observed widely in neurodegenerative conditions (Akbar et al. 2016). Pathological mitochondrial fragmentation is present in commonly used animal models of neonatal HI brain injury (Baburamani et al. 2015; Akbar et al. 2016). As metabolic deficits are found in the areas that will develop damage over time in the neonatal brain after

HI, targeting mitochondrial function seems a likely avenue for neuroprotection (Blennow et al. 1995; Blomgren and Hagberg 2006).

Beyond their role in energy metabolism, the mitochondria lie at the crux of life and death within the cell, as several cell death pathways converge and initiate at the organelle. The translocation of factors localized at the mitochondria, such as cytochrome c (cyt c) and apoptosis-inducing factor (AIF), is a precursor to apoptotic cell death. Oxidative stress after HI tips the balance of the Bcl-2 family that acts as competition to regulate mitochondrial membrane permeability that controls the subsequent release of apoptotic factors (Suen et al. 2008; Thornton et al. 2012). Apoptosis is developmentally upregulated in the neonatal brain, and any shift towards apoptotic signaling leads to exacerbated cell death in comparison to the adult brain. This is driven by several factors that ultimately culminate in a unique sensitivity to ischemic insult. Ca^{2+} over-influx is a powerful stimulus to both apoptotic and necrotic cell deaths, and is exacerbated by developmental upregulation of NMDA receptors. Likewise, several apoptotic factors such as caspase-3 and Apaf-1 are far more prevalent in the neonatal brain, as programmed cell death is critical for neural development. This is exacerbated by elevated mitochondrial release of cyt c in the neonate. Cyt c, once translocated to the cytosol, binds to Apaf-1, activating it and forming a structure called the apoptosome. Formation of this complex induces the cleavage of bound procaspase-9 to its active form. Activated caspase-9 activates caspase-3, the final “executioner” caspase, via cleavage and initiates a cascade of proteolytic degradation of cellular components, culminating in characteristic apoptotic cell death (Elmore 2007). Due to the pivotal place of the mitochondria in this process, it follows that mitoprotective strategies may improve the condition of the neonatal brain after HI injury, in part, by ameliorating neuronal cell death.

Currently, the only approved treatment for HIE is therapeutic hypothermia (TH). TH, however, has significant limitations regarding application and efficacy (Nolan et al. Nolan 2008; Kim et al. 2012; Datta 2017). TH is a therapeutic strategy practiced in HIE and cardiac arrest, wherein the body temperature of the patient is lowered with specialized equipment to a range of 32–34 °C for a duration of 12–24 h (Kim et al. 2012; Datta 2017). Although TH does have protective effects against HI damage, its application is limited by a tight time window within which TH is efficacious. TH must be administered within hours of birth, delivering diminishing returns as the time between HI insult and medical intervention increases. Beyond this, TH, even when deployed successfully, is of limited efficacy, and comes with the potential for adverse cardiovascular effects (Kim et al. 2012). These factors, taken together, necessitate the development of new therapeutic options that can be implemented within a longer timeframe and with greater efficacy to serve the needs of patients and their families.

One emerging therapeutic method targeting the mitochondria lies in photobiomodulation (PBM). Shortly after the development of laser technology, it was applied to biological systems wherein it was first discovered to accelerate hair growth and was soon applied to several biological systems. In recent years, PBM has been applied to multiple brain injury models, facilitated by the penetrance of near-infrared (NIR) wavelengths through biological tissue, including the skull of both rodents and humans. The deep penetrating range of NIR light depends on the gap between the absorption spectra of water and biological chromophores (Chung et al. 2012). PBM has shown protective properties against mitochondrial dysfunction and neuronal cell death in animal models of stroke, Alzheimer's disease (AD), Parkinson's disease (PD), and traumatic brain injury (TBI), although these benefits have yet to be successfully translated to the clinic (Zivin et al. Zivin 2009; Chung et al. 2012; Oron and Oron 2016; Xuan et al. 2016; Berman et al. 2017; Lee et al. 2017). While the mechanisms underlying PBM are largely unknown, current knowledge posits that it depends on stimulation of mitochondrial function, with cytochrome c oxidase (CCO) being the primary acceptor of light (Chung et al. 2012). Previous studies by our lab in other models have shown that PBM stimulation results in immediate and long-lasting increases in ATP production and mitochondrial function, as well as significant resistance to oxidative stress. As such, we hypothesize that PBM will provide neuroprotection against neonatal HI via promotion of mitochondrial function and preservation of healthy mitochondrial dynamics.

Materials and Methods

Experimental Design and Neonatal Rat HI Model

A modified version of the Rice-Vannucci model (Rice et al. Rice 3rd et al. 1981) was used in this study. Postnatal (P) 10 pups were assigned to 3 groups ($N=6-12$ /group): (1) Sham HI, (2) HI+sham PBM, and (3) HI+PBM. This model begins with unilateral permanent occlusion of the right common carotid artery. Unsexed P10 pups were separated from their dam and inhaled isoflurane anesthesia was induced and maintained throughout the surgical procedure. Body temperature was maintained throughout surgery and recovery at 37 °C via a heating pad and measured via rectal thermometer. An incision was made along the front of the neck, and the right common carotid was exposed. Nerve bundles were gently separated, and the artery was tightly occluded with surgical twine. The wound was closed via surgical glue, subdermal buprenorphine was administered, and the animal was returned to the dam for a 1-h recovery. After this period, pups were placed in a sealed 2-l bag filled with a hypoxic atmosphere (6% O₂ balanced with N₂) for approximately 2 h, with the body temperature

maintained by placing the hypoxia bags in a heated water bath maintained at 37 °C. Pups were then removed from the hypoxia bag, labeled, and returned to their dam. All procedures were approved by the local ethical committee and were in accordance with the National Institutes of Health guidelines. All efforts were made to minimize the suffering and the number of pups used in the surgical and experimental procedures. The protocol for induction of the HI model, PBM treatment, behavioral test, and tissue collection is shown in the experimental design (schematic diagram Fig. 1).

Photobiomodulation (PMB) Treatment

Transcranial PBM treatment was administered via a continuous wave diode laser with a wavelength of 808 nm (808M100, Dragon Lasers), as described in our previous work (Lu et al. 2017). Laser radiation was focused into a 1-cm² round spot with an expanding lens and a fiber optic cable and delivered transcranially by centering the beam 3 mm posterior from the eyes and 2 mm anterior from the ears. All treatments were performed while the animal is briefly restrained in a transparent DecapiCone (DCL-120, Braintree Scientific), including control treatment animals. Laser power was adjusted to yield a cortical power density of 25 mW/cm². Treatment was maintained for 2 min once daily for 7 days, delivering a daily dosage of 3 J/cm² at the cerebral cortex tissue level (calculated by total irradiated time (seconds) × power output (mW/cm²)/1000, expressed as J/cm²). After treatment, rats were gently removed from the DecapiCone and returned to their home cage. Two laser power meters (#FM33-056, Coherent Inc., USA and #LP1, Sanwa, Japan) were used to measure the power density passing through the skullcap and scalp placed under a section of the DecapiCone. Settings were recorded and used across experiments. Periodically, these measurements were taken again to account for power drift inherent in laser systems.

Histological Evaluation

Histological examination of brain tissue loss and neuronal survival and death was conducted by cresyl violet staining and terminal deoxynucleotidyl transferase dUTP nick end labeling (TUNEL), as described previously (Zhang et al. 2009; Ahmed et al. 2016; Ahmed et al. 2017). Briefly, rats were anesthetized and transcardially flush-perfused with ice-cold saline and fixed with 4% paraformaldehyde (PFA). The rat brains were embedded in OCT compound (Tissue-Tek) and coronal sections (25 μm thick) were obtained on a Leica Cryostat (Leica Microsystems). Brain sections were washed with 0.4% Triton X-100 in PB and stained with cresyl violet (0.01% w/v) for 10 min, followed by graded ethanol dehydration and covering slide. The stained sections were examined, and images were captured using light microscopy. The mean infarct area was calculated according to the following formula:

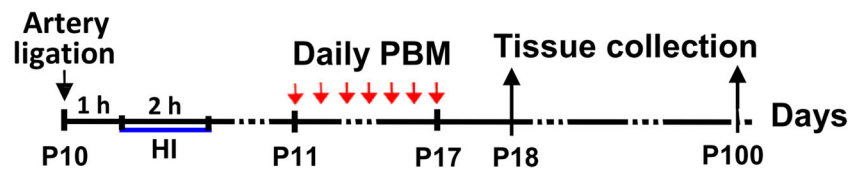


Fig. 1 Experimental design. Timepoints of hypoxic ischemia (HI) induction, photobiomodulation (PBM) treatment, and tissue collection are shown

infarct size = (area of contralateral hemisphere – area of ipsilateral hemisphere) / area of contralateral hemisphere \times 100%. To examine relative neuronal density, the numbers of surviving neurons in the area (200 μ m \times 200 μ m square) of the medial CA1 pyramidal layers and somatosensory (S1) cortex were counted from three to five representative sections of each animal (> 100 μ m gap between each section in the coronal plane, \sim 2.5–4.5 mm posterior from Bregma). Intact, normal-appearing neurons displaying around the soma and distinct stained nuclei, as appear in sham animals, were counted as surviving neurons. Neurons with abnormal-appearing, condensed, pyknotic, and shrunken nuclei were judged as dead ones. TUNEL labeling was performed on brain sections using a Click-iT® Plus TUNEL assay kit (Thermo Fisher Scientific) following the manufacturer's instructions, and the images were captured using a Zeiss LSM700 Meta confocal microscope (Carl Zeiss). The number of TUNEL-positive cells in the examined areas (200 μ m \times 200 μ m) was counted and data were presented as mean \pm standard error (SE) ($N = 8$ –12) from independent animals in each group.

Immunofluorescence Staining and Confocal Microscopy

Immunofluorescence staining was performed using standard protocol as previously described (Zhang et al. 2013; Lu et al. 2017). In brief, sections were washed with 0.4% Triton X-100 and blocked in 10% donkey serum followed by incubation with primary antibodies overnight at 4 °C. The following primary antibodies were used in this study: anti-Tom20 (Proteintech group), anti-phospho-Histone H2A.X Ser139 (cell signaling), anti-NeuN (Millipore), anti-4-Hydroxynonenal (4-HNE), and anti-Malondialdehyde (MDA) from Abcam Inc. Sections were then washed and incubated with appropriate Alexa Fluor donkey anti-mouse/rabbit secondary antibodies (Invitrogen) for 1 h, washed, coverslipped, and sealed in VECTASHIELD mounting medium with 4,6-diamidino-2-phenylindole (DAPI) (Vector Laboratories). To determine the level of total mitochondrial fragmentation, the acquired images of Tom20 fluorescent were thresholded, filtered (median, 2.0 pixels), and binarized, using ImageJ software (NIH image program, version 1.49). The counts of total mitochondrial fragmentation were defined by normalization of the number of total mitochondrial particles to total mitochondrial areas, as described in our recent work (Lu et al. 2017). To determine the depolarization level

of mitochondrial membrane potential (MMP), MitoTracker Red CMXRos (100 μ l, 50 ng/ml, Life Technologies) was administered via tail vein injection 5 min before tissue collection, as described in our previous work (Lu et al. 2016). All the fluorescence images were captured on LSM700 confocal laser microscope and analyzed using Image J software.

Brain Tissue Homogenates

As described previously (Han et al. 2015), animals were sacrificed under deep anesthesia from the sham and HI groups at P18. Brain tissues of the cortex (S1) and hippocampal CA1 regions were quickly separated and frozen in dry ice. Brain tissues were then homogenized using a Teflon homogenizer in ice-cold homogenization buffer containing 50 mM of HEPES (pH 7.40), 150 mM of NaCl, 12 mM of β -glycerophosphate, and inhibitor cocktails of proteases and enzymes (Thermo Scientific). The homogenates were vigorously mixed for 20 min on a rotator and centrifuged at 15,000 \times g for 30 min at 4 °C to yield total protein in the supernatants. Protein concentrations were determined using a Modified Lowry Protein Assay Reagent Kit (Pierce).

Quantification of ATP Production Levels

To investigate the changes of mitochondrial function after PBM treatment, the levels of ATP concentration were determined using an ENLITEN® rLuciferase/Luciferin kit (FF2021, Promega) according to the kit protocol, as described previously (Lu et al. 2016). Briefly, total protein samples (30 μ g) were suspended in 100 μ l of reconstituted rL/L reagent buffer (pH 7.75, containing luciferase, D-luciferin, tris-acetate buffer, ethylenediaminetetraacetic acid (EDTA), magnesium acetate, bovine serum albumin (BSA), and dithiothreitol (DTT)). Light emissions at 10-s intervals were measured in a microplate luminometer (PE Applied Biosystems) and ATP content values were determined from the ATP standard curve. The final levels of ATP concentration were expressed as percentage changes compared to the sham control group.

Western Blotting and Quantification of Protein Carbonyl Content

The levels of protein carbonyls in the proteins from cortex (S1) and hippocampal CA1 at P18 were measured using an OxyBlot Protein Oxidation Detection Kit (EMD Millipore Corporation)

following the manufacturer's protocol, as described in our work (Li et al. 2018). Briefly, protein was denatured and derivatized to 2,4-dinitrophenylhydrazone (DNP) by incubation with 2,4-dinitrophenylhydrazine (DNPH). Electrophoresis was performed on 4–20% SDS-PAGE and proteins were transferred to PVDF membranes. The membranes were then probed with anti-DNP primary antibody, followed by incubation with HRP-conjugated secondary antibody. Bound antibodies were visualized using enhanced chemiluminescence (ECL) method under ImageQuant LAS 4000 (GE Healthcare). The membranes were then reprobed with an anti- β -actin antibody (Proteintech Group). The level of protein carbonylation, representing oxidative stress status, was normalized to the corresponding loading controls and expressed as percentage changes versus the sham control group.

Measurement of Caspase-9 and Caspase-3 Activity

As described previously by our laboratory, caspase-9 and caspase-3 activity was measured by incubation of the protein fluorometric substrates Ac-DEVD-AMC and Ac-LEHD-AMC, respectively (Lu et al. 2016). Briefly, the reaction was initiated by mixing an equal amount of the proteins (30 μ g) from the cortex (S1) and hippocampal CA1 with a specific substrate in the assay buffer and incubated for 1 h at 37 °C. The fluorescence of free AMC, corresponding to the proteolytic activity of caspase, was measured on a spectrophotometer (Perkin Elmer). Relative caspase activity in each sample was expressed as the changes of fluorescent units and compared between groups.

Data Analysis

Data were expressed as means \pm SE and analyzed using the SigmaStat software (Systat Software). Statistical analyses were carried out using one-way analysis of variance (ANOVA), followed by Student-Newman-Keuls (SNK) post hoc tests to determine group differences. When only two groups were compared, a Student's *t* test was performed to detect significant changes following treatment. Statistical significance was accepted at the 95% probability value (corresponding to $P < 0.05$).

Results

PBM Treatment Decreased Hemispheric Brain Shrinkage and Neuronal Cell Death Induced by HI Insult

Neonatal hypoxic-ischemic (HI) brain injuries invoke pronounced neuronal death and glial activation and lead to secondary maturational disturbances. These neuropathological

features are pronounced in specific brain regions, including the sensorimotor cortex and dorsal hippocampal subregions. Insult to these regions can induce subsequent sensory and motor dysfunction, as well as learning and attentional deficits (van de Looij et al. 2014). In the current study, the neuronal morphology of sensorimotor cortex and hippocampal CA1 regions was examined on both early timepoint (P18) and late timepoint (P100) after HI via Nissl staining. As shown in Fig. 2A, neonatal rats subjected to HI insult displayed dramatic neuronal death in the cortex and hippocampal CA1 regions on both P18 and P100, which was strongly attenuated by PBM treatment. Further quantitative analysis revealed that the loss of ipsilateral brain tissue in HI rats was approximately 17% on P18 and 32% on P100 after HI injury. PBM, however, reduced brain loss at the aforementioned timepoints to 5% and 12%, respectively (Fig. 2B). This robust preservation of brain volume is indicative of both short-term and long-term protective effects. Further analysis for relative neuronal density suggested that PBM treatment also dramatically rescued the decreased neuronal density in both the cortex and hippocampal CA1 regions of HI rats, as shown in Fig. 2C.

PBM Treatment Suppressed HI-Induced Mitochondrial Fragmentation

Ischemic neuronal death has been demonstrated to involve the imbalance of mitochondrial dynamics, characterized by mitochondrial fragmentation. As a critical organelle that maintains neuronal survival, mitochondrial dysfunction will initiate mitochondria-dependent apoptotic signaling pathway, and accelerate downstream cell death cascade. Therefore, mitochondria-targeted strategies might be effective on the attenuation of HI injury. To examine mitochondrial morphology in the cortex and hippocampal CA1 regions from P18 rats, immunofluorescence imaging of Tom-20 was carried out, and the segments were further separated, thresholded, filtered, and binarized using Image J software. Mitochondria in both the cortex (Fig. 3A) and hippocampal CA1 (Fig. 3B) regions of HI rats displayed a significantly higher degree of fragmentation than sham control. In contrast, PBM treatment profoundly relieved the mitochondrial fragmentation to a degree that is comparable to that observed in sham animals. This result indicates a crucial ability of PBM intervention on mitochondrial integrity by maintaining a healthy balance of mitochondrial fission and fusion processes, which may indicate a potent mechanism for neuronal survival in the context of HI brain injury.

PBM Treatment Attenuated Mitochondrial Dysfunction Induced by HI

Mitochondrial dysfunction and energy failure play a pivotal role in the development and progression of ischemic brain

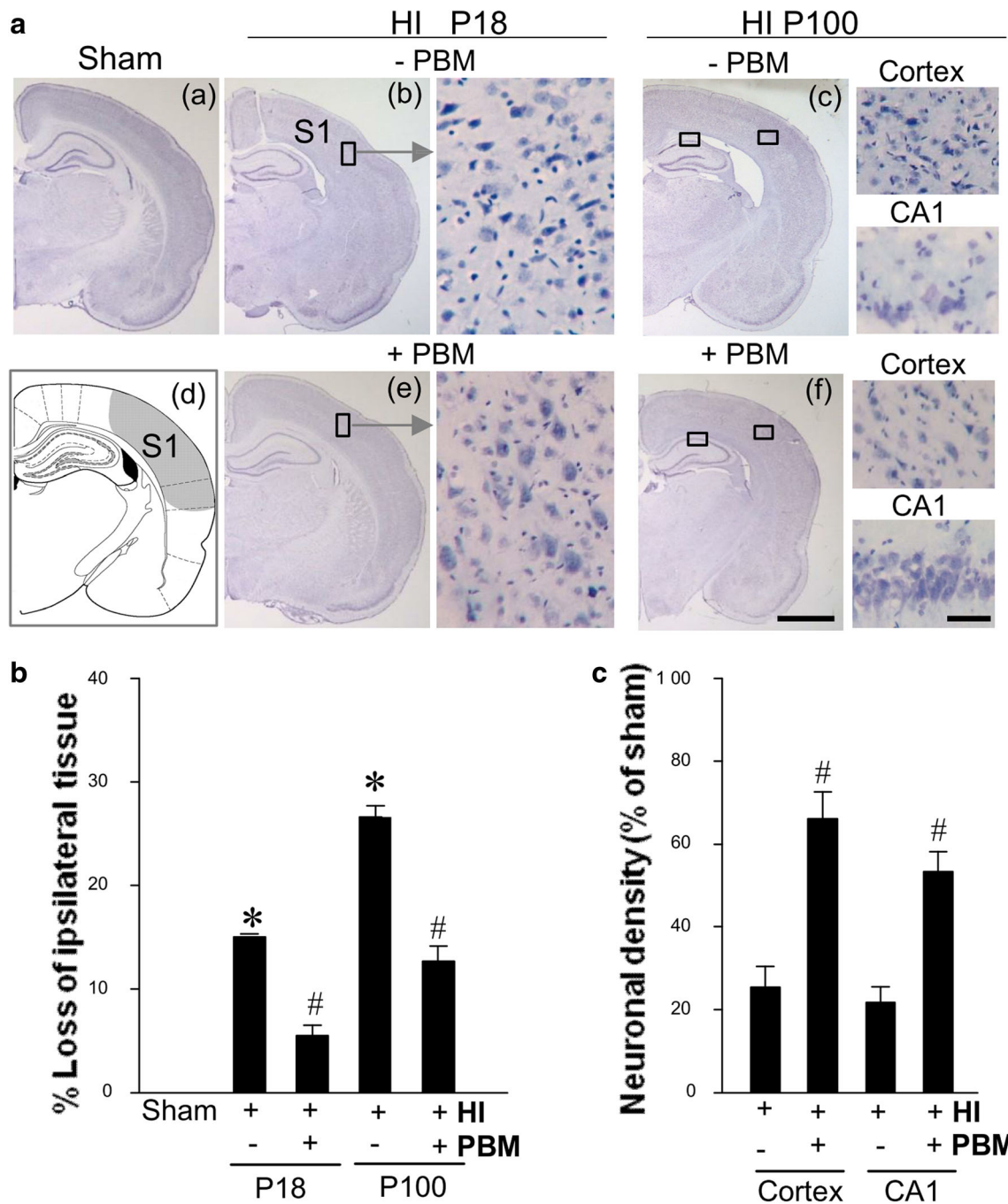


Fig. 2 PBM treatment reduced hemispheric brain tissue loss and neuronal death. **A** Brain tissues were examined on both P18 and P100 after HI. Location of somatosensory (S1) cortex is shown in (d). **B, C** Brain damage was evaluated by calculation of the loss of ipsilateral tissue (at p18 and p100) and relative neuronal density (at p100) in the cortical

infarct area and damaged hippocampal CA1 region ($N = 8-12$). Scale bar: 500 μm (in the overview) and 50 μm (in the enlarged area). * $P < 0.05$ versus sham, # $P < 0.05$ versus HI control group without PBM treatment

injury and neuronal death. As a critical organelle that maintains neuronal survival, mitochondrial dysfunction can initiate mitochondria-dependent apoptotic signaling pathway, accelerating downstream cell death cascades. Therefore, mitochondria-targeted strategies may prove effective in attenuating short-term and long-term HI injuries. To investigate mitochondrial dysfunction, functionally critical mitochondrial

membrane potential (MMP) was examined in P18 animals, with MitoTracker Red fluorescent dye, a marker of MMP. Confocal images of MitoRed staining in Fig. 4A, B and further quantitative analysis in Fig. 4C revealed drastic decreases in the MitoTracker Red signal of both the cortex and hippocampal CA1 neurons from HI rats compared with sham control. PBM treatment, in contrast, strongly reversed the trend of

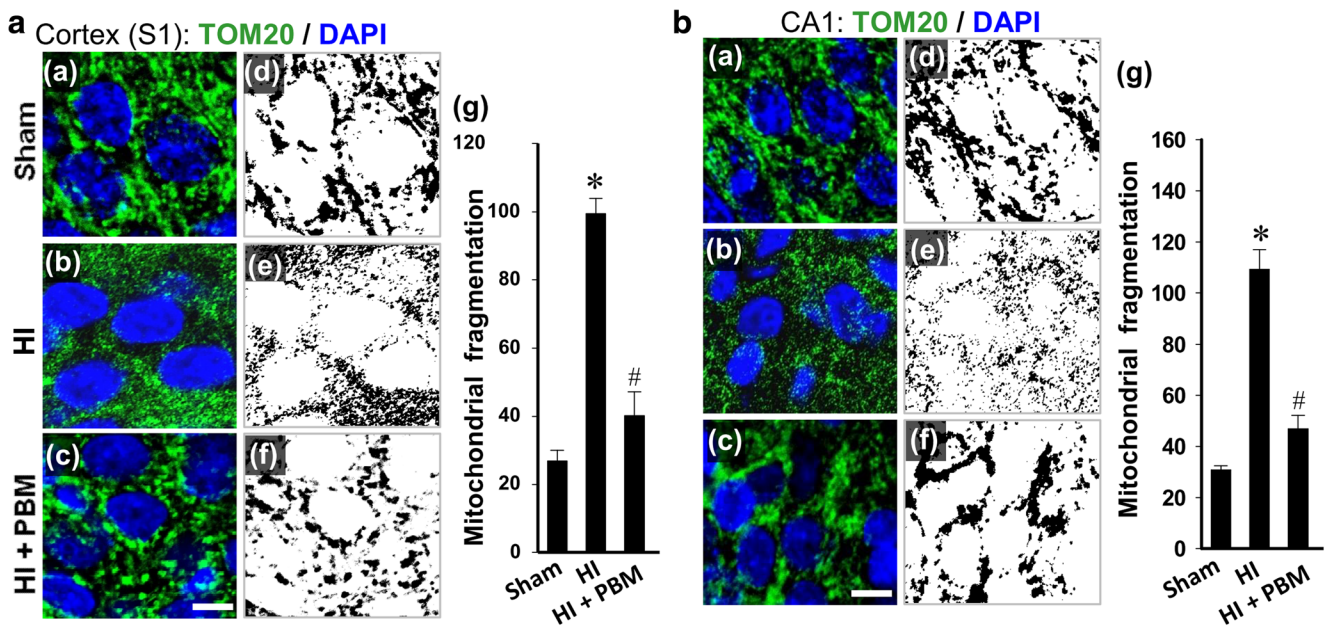


Fig. 3 Effect of PBM treatment on HI-induced changes in mitochondrial fragmentation of cortex and hippocampal pyramidal neurons. **A, B** (a–c) Representative immunofluorescence images of Tom20 staining (green) counterstained with nuclear marker DAPI (blue) of the cortex (S1) and hippocampal CA1 neurons from P18 animals. Scale bar: 5 μ m. **A, B** (d–g) The immunofluorescence of Tom20 was separated, thresholded,

filtered, and binarized using the Image J program. The counts of total mitochondrial fragmentation were calculated by normalization of the number of total mitochondrial segments to total mitochondrial areas. Data are presented as means \pm SE ($N=4-6$ in each group). * $P < 0.05$ versus sham HI control, # $P < 0.05$ versus HI or HI + sham PBM group

decreased fluorescent signal in HI rats, suggesting significant attenuation of mitochondrial MMP collapse. Next, ATP production was measured in total protein fraction samples from both the cortex and the hippocampal CA1 subregions. As shown in Fig. 4D, rats subjected to HI insult displayed remarkable ATP decline in both regions, which was potentially reversed by PBM treatment. Taken together, these results demonstrated a robust ameliorating effect of PBM intervention on HI-induced mitochondrial dysfunction in neonatal rats.

PBM Treatment Abated Oxidative Damage in the HI Infarct Brain

Evidence has accumulated, from our studies and others, which suggests that neonatal hypoxia-ischemia injury induces long-lasting oxidative stress, a process exacerbated by mitochondrial dysfunction (Odorcyk et al. 2017; Zhang et al. 2018). The positive effect of PBM treatment on mitochondrial function demonstrated above leads us to hypothesize that HI-triggered oxidative damage to cellular components in neonatal rats may be attenuated by PBM intervention. First, oxidative damage in the S1 cortex was investigated by measuring the markers of lipid peroxidation (4-HNE) and DNA double-strand breaks (P-H2A.X), as shown in Fig. 5A. In agreement with the inhibitory effect on mitochondrial dysfunction, PBM was shown to markedly reduce the HI-induced surge of both 4-HNE and P-H2A.X expressions. Similar results were found

in the hippocampal CA1 subregion after staining for MDA, another widely used marker of lipid peroxidation (Fig. 5B). Finally, we measured levels of protein carbonyls generated from oxidative damage to cellular proteins via Western blot analysis (Fig. 5C). Quantitative analysis indicated that protein carbonyl production in both the cortex and hippocampal CA1 infarct regions was profoundly suppressed by PBM treatment, further indicating the ability of PBM to decrease HI-induced oxidative damage.

PBM Treatment Suppressed Activation of Caspase-9/Caspase-3 Apoptotic Pathway in HI Rats

It is well established that HI insult leads to activation of mitochondria-dependent caspase-9/caspase-3 apoptotic pathway in neonatal rats. Therefore, we next measured the anti-apoptotic effect of PBM treatment in HI infarct brains. As shown in Fig. 6A, B, fluorometric substrate assays for samples taken from the cortex and hippocampal CA1 regions at P18 revealed that HI induced a remarkable increase in the activity of pro-apoptotic proteins caspases 9 and 3. This effect was sharply blunted by PBM treatment. Finally, apoptosis in both infarct regions was examined using TUNEL staining. As shown in Fig. 6C, D, HI rats consistently displayed robust increases in TUNEL-positive cells compared with sham control animals, which was dramatically attenuated by PBM treatment.

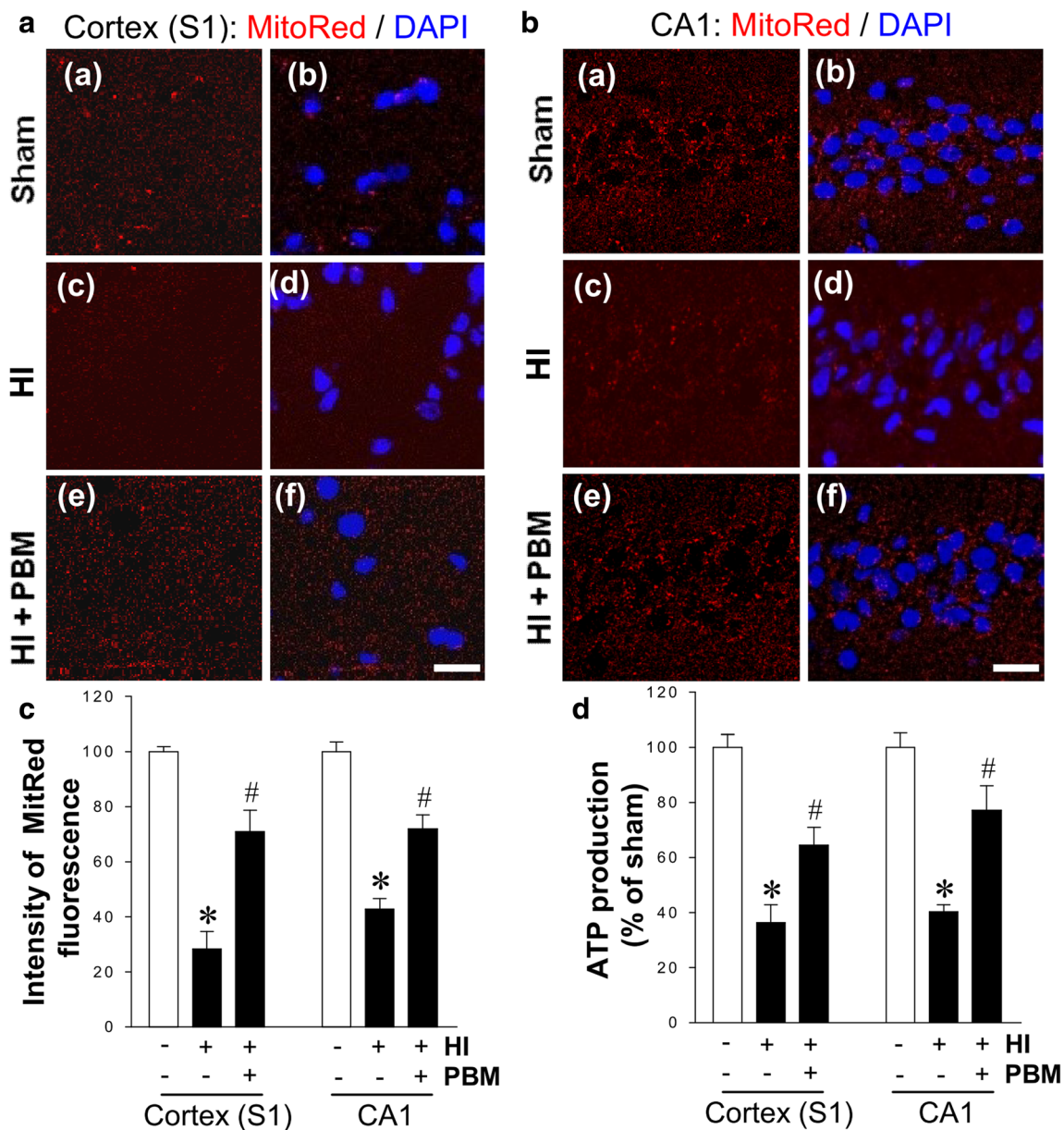


Fig. 4 Effect of PBM treatment on HI-induced mitochondrial dysfunction in the infarct brain. **A, B** Representative microscopic images of MitoTracker Red immunofluorescence in cortex (S1) and hippocampal CA1 neurons from P18 animals. The tissue sections were counterstained with DAPI. Scale bars = 20 μ m. **C** The intensity level of MitoTracker fluorescence associated with MMP was determined and

expressed as percentage changes compared with the sham group. **D** The level of ATP production was detected in the indicated protein samples from each group at P18 and the value was compared within groups. * $P < 0.05$ versus sham, # $P < 0.05$ versus HI control group without PBM treatment. Data are means \pm SE from 4 to 6 animals in each group

Discussion

Perinatal hypoxic-ischemic encephalopathy (HIE) is one of the leading contributors to mortality in neonates, leading to long-term neurological disability and pathologies, such as spasticity, cognitive impairment, sensory deficits, and motor abnormality (Vannucci et al. 1999; Kim et al. 2017). Despite years of investigation, treatment for HIE remains extremely limited. In the current study, we demonstrated for the first time that PBM treatment exerts a beneficial

effect on a wide breadth of HIE pathological analogues in the neonatal HI rat model. PBM had pronounced effects on cerebral infarct size and neuronal cell death in the cortex and hippocampal CA1. In line with the proposed mechanisms of PBM, posttreatment with PBM suppressed HI-induced mitochondrial dysfunction and fragmentation and consequent oxidative neuronal damage. These results provide insight into protective mechanisms of a novel treatment paradigm for neonatal HI injury that could offer recovery for those affected by HIE.

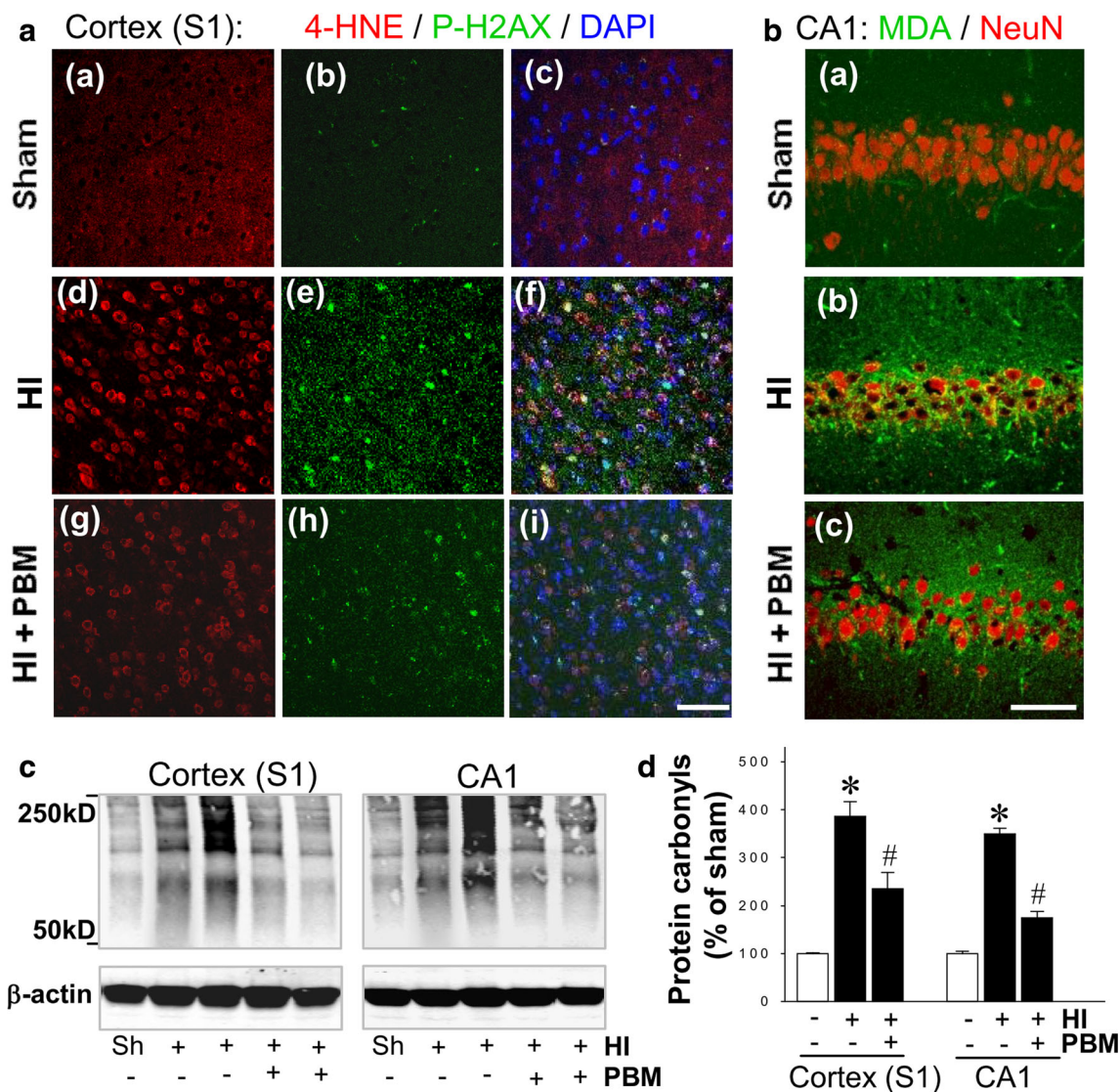


Fig. 5 Effect of PBM treatment on HI-induced oxidative damage in the infarct brain. **A, B** Representative microscopy images of the damaged brain regions showing the staining of 4-HNE, P-H2AX (S139), DAPI, malondialdehyde (MDA), and NeuN at P18 from each group. Scale bars = 50 μ m. **C, D** The level of protein carbonyls, representing

oxidative stress, was measured at P18 using a protein carbonyl content assay kit and Western blotting. Data are means \pm SE (N = 4–6) expressed as percentage changes versus sham control group. * P < 0.05 versus sham, # P < 0.05 versus HI control group

HI injury has been demonstrated to exact particular damage to the cerebral cortex and dorsal hippocampus, which accounts for the high frequency of locomotor and cognitive deficits in neonates suffering from HIE (McQuillen et al. 2003; Albrecht et al. 2005). Clinical studies on human preterm infants with electroencephalogram (EEG) revealed reduced background activity, which can be used as sensitive marker of damaged cortical circuits (Toet et al. 1999). Reduced dendritic spine maturation and synapse formation of cortical neurons is a further indicator of future sensorimotor deficits. As well, learning and memory impairment is a common clinical characteristic that follows for a lifetime those who survive the initial HI insult. The dorsal hippocampus, the CA1 region in particular, is frequently studied due to its critical role in

learning and memory (Goodrich-Hunsaker et al. 2008). Accordingly, our study demonstrated that HI injury in neonatal rats caused profound ipsilateral brain lesions in both the cortex and hippocampal CA1 regions, observed at both P18 and P100. PBM treatment has been well-documented to impart a protective effect on neurodegenerative diseases by our lab and others in conditions such as AD, stroke, and aging (Lu et al. 2017; Salehpour et al. 2017; Yang et al. 2018). The current work corroborates this by demonstrating that PBM intervention at the early stage of neonatal HI injury exhibits pronounced effects on the preservation of brain lesion volume, both over the short-term and long-term time windows.

As the primary source of energy for the brain and a central hub for cell death signaling, mitochondria play a critical role

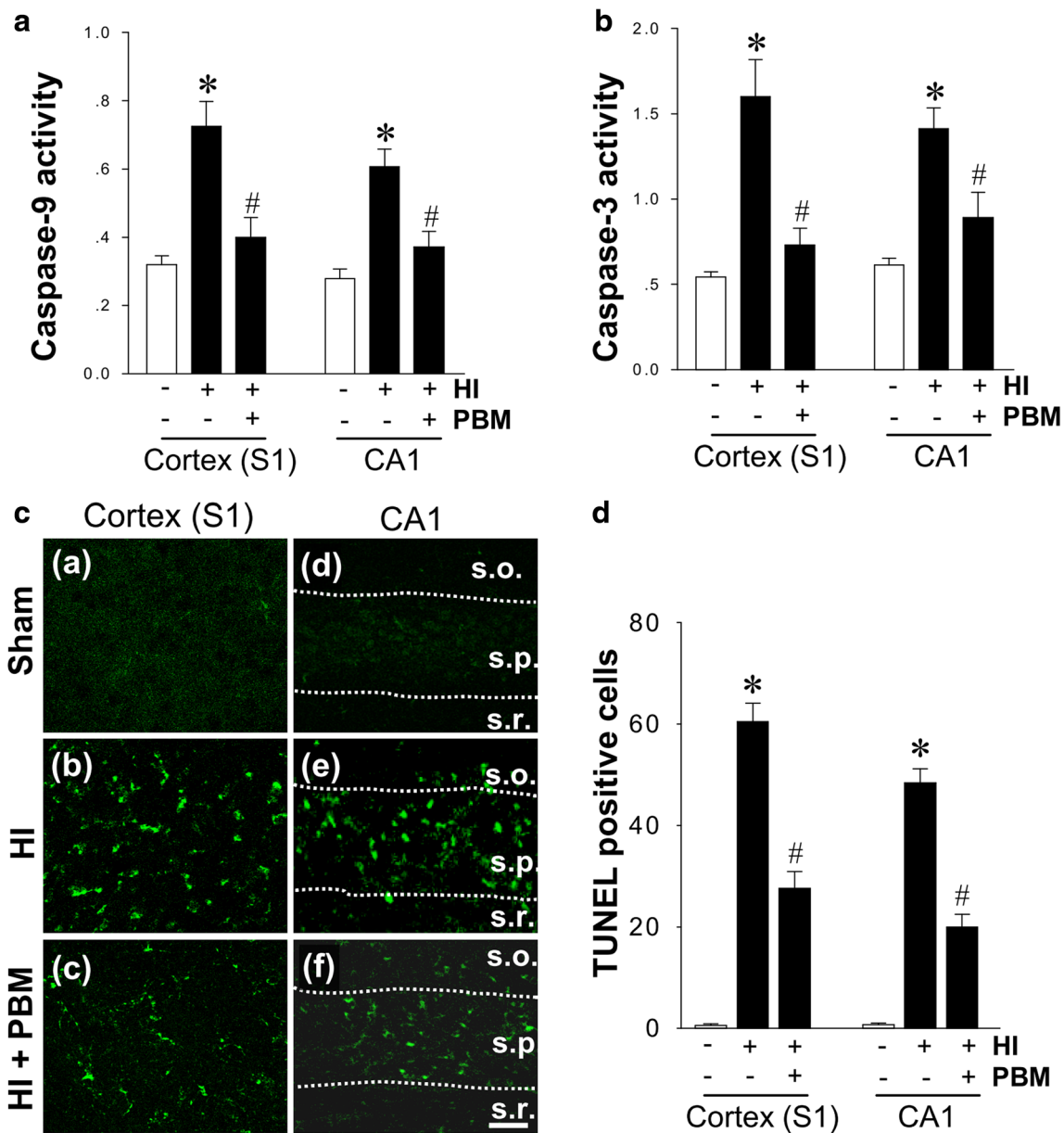


Fig. 6 Effect of PBM treatment on caspase-9 and caspase-3 activity and apoptotic cell death induced by HI. **A, B** The change of caspase-9 and caspase-3 activity in the proteins from the cortex (S1) and hippocampal CA1 was examined using specific AMC-based fluorometric substrates at P18 from the sham and HI rats. The fluorescence of free AMC was measured and compared between groups. **C** Representative confocal microscopy images depict fluorescent TUNEL staining (green) in the

cortex (S1) and hippocampus CA1 regions (s.o., stratum oriens; s.p., stratum pyramidale, and s.r., stratum radiatum). Scale bar: 20 μ m. **D** The numbers of TUNEL positive cells from the indicated groups were counted and statistically determined. Results are means \pm SE from four to five animals in **(A)** and **(B)**, and 8–12 animals in **(C)** and **(D)** in each group. * $P < 0.05$ versus sham, # $P < 0.05$ versus HI control group

for cell survival. Mitochondrial dysfunction caused by ischemic insult causes primary energetic failure and initiates a battery of self-perpetuating pathological events that ultimately lead to neuronal degeneration and apoptosis, in part mediated by excessive generation of reactive oxygen species (Akbar et al. 2016; Ham and Raju Ham 3rd and Raju 2017). This process causes long-term damage that prolongs the impact of the initial insult, causing deficits in energy production and disruption of mitochondrial dynamics, as preservation of

mitochondrial integrity is associated with structural dynamics by balancing fission and fusion processes (Bertholet et al. 2016). The dynamic balance of mitochondrial fission and fusion can determine their morphology and enable quick adaptation for energetic needs, as well as maintaining mitochondrial integrity. These processes are controlled by a series of factors, primarily GTPases, i.e., DRP1, FIS1, OPA1, and MFN1, which are located on the mitochondrial outer membrane and mediate the processes of mitochondrial fission and

fusion, respectively. Disturbances in the expression, integrity, and function of these proteins are present in several neurodegenerative disorders. Mitochondrial fragmentation, in particular, is a characteristic hallmark in the pathogenesis of many of these diseases, and is, in part, triggered by the overproduction of fission-related proteins (Otera et al. 2013; Chao de la Barca et al. 2016). Following these detrimental morphological alterations, mitochondria undergo exacerbated functional compromise, characterized by declining mitochondrial membrane potential and ATP synthesis deficits. In the current study, we observed that unilateral HI insult to neonatal rats induced significant mitochondrial abnormalities, including extensive mitochondrial fragmentation and subsequent decline in energy production. PBM treatment, however, managed to facilitate ATP production and reversed the trend of mitochondrial fragmentation, a beneficial effect which has been consistently demonstrated in our previous studies involving different neurodegenerative models (Lu et al. 2017; Xu et al. 2017).

Evidence has shown that oxidative stress is a critical mechanism for the development of HI brain injury, and it is strongly linked with alterations and dysfunction of mitochondrial respiratory complexes I and IV activity (Wyatt 1994; Niatsetskaia et al. 2012; Sosunov et al. 2015). Mitochondrial dysfunction leads to a buildup of radical oxidative species via electron leakage, which can feedback and exacerbate mitochondrial impairment through damage to critical mitochondrial components. This damage spills out from the mitochondria into other cellular compartments, causing irreversible damage to critical cellular macromolecules (Akbar et al. 2016; Ham and Raju Ham 3rd and Raju 2017). The brain tissue, because of its high level of lipid content, is thus particularly vulnerable to the ravages of oxidative damage (Wang et al. 2014). In this work, we demonstrated that PBM was able to exert robust anti-oxidative effects in the cortex and hippocampal CA1 regions, in line with our results regarding mitochondrial function. This was expressed by a sharp decrease in markers of lipid, DNA, and protein oxidative damage. By protecting against this damage and the subsequent signaling cascade, we believe that PBM mitigates the excessive cell death that follows HI insult and contributes to HIE pathology.

Following mitochondrial damage and resultant oxidative stress, mitochondrial dependent apoptotic pathways are activated. This is initiated by cyt c release, followed by formation of the apoptosome and activation, via proteolytic cleavage, of caspase-3 and caspase-9, triggering an irreversible cascade leading to cell death (Lu et al. 2015). This process is particularly dramatic in the neonatal brain due to developmentally appropriate upregulation of apoptotic factors and their release, as well as a general sensitivity to oxidative stress (Thornton et al. 2012). This death is pronounced in critically sensitive neuronal progenitor pools and oligodendrocyte progenitors, contributing heavily to the developmental deficits and

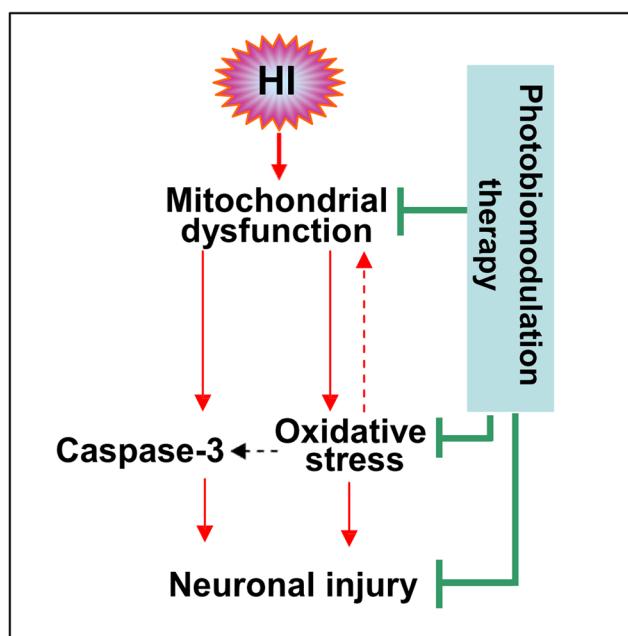


Fig. 7 Schematic summary of the neuroprotective effect of photobiomodulation therapy. HI-induced mitochondrial dysfunction contributes to oxidative stress and caspase-3 activation, resulting in neuronal cell death (apoptosis) in the cortex (S1) and hippocampal CA1 regions. Oxidative stress can further attack mitochondria in a positive-feedback manner. Photobiomodulation therapy was able to attenuate these detrimental effects and improve neuronal survival

morphological abnormalities underlying HI injury in the neonatal brain (Vannucci and Hagberg 2004). TUNEL staining revealed dramatic increases in the levels of neuronal apoptosis in the cortex and hippocampal CA1, as observed at P18. PBM attenuated this apoptosis, ameliorating the HI-induced damage. In line with these results, fluorometric substrate assays uncovered a striking upregulation in the activity of pro-apoptotic proteins caspase-3 and caspase-9 in HI infarct brains. This surge in apoptotic signaling was countered by PBM treatment, potentially accounting for the decrease in neuronal apoptotic cell death.

In conclusion, the current study demonstrates the profound neuroprotective effects of PBM treatment on HI injury in neonatal rats. We believe that these effects are a result of, in part, preservation of mitochondrial function and suppression of HI-induced oxidative stress. The result of this is a marked suppression of apoptotic signaling and neuronal cell death, which translates into protection against long-lasting hemispheric shrinkage that is characteristic of brain injury in the hypersensitive perinatal period (Fig. 7). Taken together, our findings provide evidence of the efficacy of PBM as a novel non-pharmacological therapeutic option in the management of HI injury that can supplement the limited treatment options that are currently available. We believe that PBM, if successfully translated to the clinic, may help those affected by HIE reach their full potential and spare patients and their families the undue suffering HIE inflicts.

Funding Information This study was supported by Research Grant NS086929 from the National Institute of Neurological Disorders and Stroke, National Institutes of Health, USA.

Compliance with Ethical Standards

All procedures were approved by the local ethical committee and were in accordance with the National Institutes of Health guidelines. All efforts were made to minimize the suffering and the number of pups used in the surgical and experimental procedures.

Conflict of Interest The author declares that there is no conflict of interest.

References

- Ahmed ME, Tucker D, Dong Y, Lu Y, Zhao N, Wang R, Zhang Q (2016) Methylene blue promotes cortical neurogenesis and ameliorates behavioral deficit after photothrombotic stroke in rats. *Neuroscience* 336:39–48
- Ahmed ME, Dong Y, Lu Y, Tucker D, Wang R, Zhang Q (2017) Beneficial effects of a CaMKII α inhibitor TatCN21 peptide in global cerebral ischemia. *J Mol Neurosci*: MN 61:42–51
- Akbar M, Essa MM, Daradkeh G, Abdelmegeed MA, Choi Y, Mahmood L, Song BJ (2016) Mitochondrial dysfunction and cell death in neurodegenerative diseases through nitroxidative stress. *Brain Res* 1637:34–55
- Albrecht J, Hanganu IL, Heck N, Luhmann HJ (2005) Oxygen and glucose deprivation induces major dysfunction in the somatosensory cortex of the newborn rat. *Eur J Neurosci* 22:2295–2305
- Baburamani AA, Hurling C, Stolp H, Sobotka K, Gressens P, Hagberg H, Thornton C (2015) Mitochondrial optic atrophy (OPA) 1 processing is altered in response to neonatal hypoxic-ischemic brain injury. *Int J Mol Sci* 16:22509–22526
- Berman MH, Halper JP, Nichols TW, Jarrett H, Lundy A, Huang JH (2017) Photobiomodulation with near infrared light helmet in a pilot, placebo controlled clinical trial in dementia patients testing memory and cognition. *J Neurol Neurosci* 8
- Bertholet AM, Delerue T, Millet AM, Moulis MF, David C, Daloyau M, Amaune-Pelloquin L, Davezac N, Mils V, Miquel MC, Rojo M, Belenguer P (2016) Mitochondrial fusion/fission dynamics in neurodegeneration and neuronal plasticity. *Neurobiol Dis* 90:3–19
- Blennow M, Ingvar M, Lagercrantz H, Stone-Elander S, Eriksson L, Forsberg H, Ericson K, Flodmark O (1995) Early [18 F]FDG positron emission tomography in infants with hypoxic-ischaemic encephalopathy shows hypermetabolism during the postasphyctic period. *Acta Paediatr* 84:1289–1295
- Blomgren K, Hagberg H (2006) Free radicals, mitochondria, and hypoxia-ischemia in the developing brain. *Free Radic Biol Med* 40:388–397
- Chao de la Barca JM, Prunier-Mirebeau D, Amati-Bonneau P, Ferre M, Sarzi E, Bris C, Leruez S, Chevrollier A, Desquiere-Dumas V, Gueguen N, Verny C, Hamel C, Milea D, Procaccio V, Bonneau D, Lenaers G, Reynier P (2016) OPA1-related disorders: diversity of clinical expression, modes of inheritance and pathophysiology. *Neurobiol Dis* 90:20–26
- Chung H, Dai T, Sharma SK, Huang YY, Carroll JD, Hamblin MR (2012) The nuts and bolts of low-level laser (light) therapy. *Ann Biomed Eng* 40:516–533
- Colver A, Fairhurst C, Pharoah PO (2014) Cerebral palsy. *Lancet* 383:1240–1249
- Datta V (2017) Therapeutic hypothermia for birth asphyxia in neonates. *Indian J Pediatr* 84:219–226
- van de Looij Y, Chatagner A, Quairiaux C, Gruetter R, Huppi PS, Sizonenko SV (2014) Multi-modal assessment of long-term erythropoietin treatment after neonatal hypoxic-ischemic injury in rat brain. *PLoS One* 9:e95643
- Elmore S (2007) Apoptosis: a review of programmed cell death. *Toxicol Pathol* 35:495–516
- Goodrich-Hunsaker NJ, Hunsaker MR, Kesner RP (2008) The interactions and dissociations of the dorsal hippocampus subregions: how the dentate gyrus, CA3, and CA1 process spatial information. *Behav Neurosci* 122:16–26
- Ham PB 3rd, Raju R (2017) Mitochondrial function in hypoxic ischemic injury and influence of aging. *Prog Neurobiol* 157:92–116
- Han D, Scott EL, Dong Y, Raz L, Wang R, Zhang Q (2015) Attenuation of mitochondrial and nuclear p38 α signaling: a novel mechanism of estrogen neuroprotection in cerebral ischemia. *Mol Cell Endocrinol* 400:21–31
- Juul SE, Ferriero DM (2014) Pharmacologic neuroprotective strategies in neonatal brain injury. *Clin Perinatol* 41:119–131
- Kim YM, Yim HW, Jeong SH, Klem ML, Callaway CW (2012) Does therapeutic hypothermia benefit adult cardiac arrest patients presenting with non-shockable initial rhythms?: A systematic review and meta-analysis of randomized and non-randomized studies. *Resuscitation* 83:188–196
- Kim HN, Pak ME, Shin MJ, Kim SY, Shin YB, Yun YJ, Shin HK, Choi BT (2017) Comparative analysis of the beneficial effects of treadmill training and electroacupuncture in a rat model of neonatal hypoxia-ischemia. *Int J Mol Med* 39:1393–1402
- Lee HI, Lee SW, Kim NG, Park KJ, Choi BT, Shin YI, Shin HK (2017) Low-level light emitting diode therapy promotes long-term functional recovery after experimental stroke in mice. *J Biophotonics* 10:1761–1771
- Li L, Yang R, Li P, Lu H, Hao J, Tucker D, Zhang Q (2018) Combination treatment with methylene blue and hypothermia in global cerebral ischemia. *Mol Neurobiol* 55:2042–2055
- Lu Y, Tucker D, Dong Y, Zhao N, Zhuo X, Zhang Q (2015) Role of mitochondria in neonatal hypoxic-ischemic brain injury. *J Neurosci Rehabil* 2:1–14
- Lu Q, Tucker D, Dong Y, Zhao N, Zhang Q (2016) Neuroprotective and functional improvement effects of methylene blue in global cerebral ischemia. *Mol Neurobiol* 53:5344–5355
- Lu Y, Wang R, Dong Y, Tucker D, Zhao N, Ahmed ME, Zhu L, Liu TC, Cohen RM, Zhang Q (2017) Low-level laser therapy for beta amyloid toxicity in rat hippocampus. *Neurobiol Aging* 49:165–182
- McQuillen PS, Sheldon RA, Shatz CJ, Ferriero DM (2003) Selective vulnerability of subplate neurons after early neonatal hypoxia-ischemia. *J Neurosci* 23:3308–3315
- Niatsetskaia ZV, Sosunov SA, Matisuevich D, Utkina-Sosunova IV, Ratner VI, Starkov AA, Ten VS (2012) The oxygen free radicals originating from mitochondrial complex I contribute to oxidative brain injury following hypoxia-ischemia in neonatal mice. *J Neurosci* 32:3235–3244
- Nolan JP et al. (2008) Post-cardiac arrest syndrome: epidemiology, pathophysiology, treatment, and prognostication. A scientific statement from the International Liaison Committee on Resuscitation; the American Heart Association Emergency Cardiovascular Care Committee; the Council on Cardiovascular Surgery and Anesthesia; the Council on Cardiopulmonary, Perioperative, and Critical Care; the Council on Clinical Cardiology; the Council on Stroke. *Resuscitation* 79:350–379
- Odorcyk FK, Kolling J, Sanches EF, Wyse ATS, Netto CA (2017) Experimental neonatal hypoxia ischemia causes long lasting changes of oxidative stress parameters in the hippocampus and the spleen. *J Perinat Med*
- Oron A, Oron U (2016) Low-level laser therapy to the bone marrow ameliorates neurodegenerative disease progression in a mouse

- model of Alzheimer's disease: a minireview. *Photomed Laser Surg* 34:627–630
- Otera H, Ishihara N, Mihara K (2013) New insights into the function and regulation of mitochondrial fission. *Biochim Biophys Acta* 1833:1256–1268
- Rice JE 3rd, Vannucci RC, Brierley JB (1981) The influence of immaturity on hypoxic-ischemic brain damage in the rat. *Ann Neurol* 9:131–141
- Rumajogee P, Bregman T, Miller SP, Yager JY, Fehlings MG (2016) Rodent hypoxia-ischemia models for cerebral palsy research: a systematic review. *Front Neurol* 7:57
- Salehpour F, Ahmadian N, Rasta SH, Farhodi M, Karimi P, Sadigh-Eteghad S (2017) Transcranial low-level laser therapy improves brain mitochondrial function and cognitive impairment in D-galactose-induced aging mice. *Neurobiol Aging* 58:140–150
- Simple BD, Blomgren K, Gimlin K, Ferriero DM, Noble-Haesslein LJ (2013) Brain development in rodents and humans: identifying benchmarks of maturation and vulnerability to injury across species. *Prog Neurobiol* 106–107:1–16
- Smith J, Wells L, Dodd K (2000) The continuing fall in incidence of hypoxic-ischaemic encephalopathy in term infants. *BJOG: Int J Obstet Gynaecol* 107:461–466
- Sosunov SA, Ameer X, Niatsetskaya ZV, Utkina-Sosunova I, Ratner VI, Ten VS (2015) Isoflurane anesthesia initiated at the onset of reperfusion attenuates oxidative and hypoxic-ischemic brain injury. *PLoS One* 10:e0120456
- Suen DF, Norris KL, Youle RJ (2008) Mitochondrial dynamics and apoptosis. *Genes Dev* 22:1577–1590
- Thornton C, Rousset CI, Kichev A, Miyakuni Y, Vontell R, Baburamani AA, Fleiss B, Gressens P, Hagberg H (2012) Molecular mechanisms of neonatal brain injury. *Neurol Res Int* 2012:506320
- Toet MC, Hellstrom-Westas L, Groenendaal F, Eken P, de Vries LS (1999) Amplitude integrated EEG 3 and 6 hours after birth in full term neonates with hypoxic-ischaemic encephalopathy. *Arch Dis Child Fetal Neonatal Ed* 81:F19–F23
- Vannucci SJ, Hagberg H (2004) Hypoxia-ischemia in the immature brain. *J Exp Biol* 207:3149–3154
- Vannucci RC, Connor JR, Mauger DT, Palmer C, Smith MB, Towfighi J, Vannucci SJ (1999) Rat model of perinatal hypoxic-ischemic brain damage. *J Neurosci Res* 55:158–163
- Wang X, Wang W, Li L, Perry G, Lee HG, Zhu X (2014) Oxidative stress and mitochondrial dysfunction in Alzheimer's disease. *Biochim Biophys Acta* 1842:1240–1247
- Wyatt JS (1994) Noninvasive assessment of cerebral oxidative metabolism in the human newborn. *J R Coll Physicians Lond* 28:126–132
- Xu Z, Guo X, Yang Y, Tucker D, Lu Y, Xin N, Zhang G, Yang L, Li J, Du X, Zhang Q, Xu X (2017) Low-level laser irradiation improves depression-like behaviors in mice. *Mol Neurobiol* 54:4551–4559
- Xuan W, Huang L, Hamblin MR (2016) Repeated transcranial low-level laser therapy for traumatic brain injury in mice: biphasic dose response and long-term treatment outcome. *J Biophotonics* 9:1263–1272
- Yang L, Tucker D, Dong Y, Wu C, Lu Y, Li Y, Zhang J, Liu TC, Zhang Q (2018) Photobiomodulation therapy promotes neurogenesis by improving post-stroke local microenvironment and stimulating neuroprogenitor cells. *Exp Neurol* 299:86–96
- Zhang QG, Raz L, Wang R, Han D, De Sevilla L, Yang F, Vadlamudi RK, Brann DW (2009) Estrogen attenuates ischemic oxidative damage via an estrogen receptor alpha-mediated inhibition of NADPH oxidase activation. *J Neurosci* 29:13823–13836
- Zhang QG, Wang RM, Scott E, Han D, Dong Y, Tu JY, Yang F, Reddy Sareddy G, Vadlamudi RK, Brann DW (2013) Hypersensitivity of the hippocampal CA3 region to stress-induced neurodegeneration and amyloidogenesis in a rat model of surgical menopause. *Brain: J Neurol* 136:1432–1445
- Zhang J, Tucker LD, Dong Yan LY, Yang L, Wu C, Li Y, Zhang Q (2018) Tert-butylhydroquinone post-treatment attenuates neonatal hypoxic-ischemic brain damage in rats. *Neurochem Int* 116:1–12
- Zivin JA et al. (2009) Effectiveness and safety of transcranial laser therapy for acute ischemic stroke. *Stroke* 40:1359–1364